Journal of Process Control 132 (2023) 103124

Contents lists available at ScienceDirect

Journal of Process Control

journal homepage: www.elsevier.com/locate/jprocont

Control of microfluidic separation processes governed by the Zweifach-Fung effect

Nicolas Petit

MINES Paris, PSL University, Centre Automatique et Systèmes, 60, bd Saint-Michel 75272, Paris, France

ARTICLE INFO

Keywords:
Microfluidics
Process control applications
Control of micro- and nano-systems
Control of particulate processes
Delay systems
Non-smooth and discontinuous optimal control problems
Prediction based control

ABSTRACT

This paper addresses several control problems for a prototypical microfluidic process designed for the separation operations of a fluid containing particles. The device is composed of one or several cascaded bifurcations that are traveled by the fluid. The volume fraction of particles in the flow is modified at each bifurcation. Fractionation is caused by the Zweifach–Fung effect, which governs the fluid dynamics in this device. It is a nonlinear effect that solely depends on the ratio of the flow rates in the branches. Propagation through the dead- volumes of the device and its capillary tubings generate input-varying delays of hydraulic type. These hydraulic delays strongly contribute to the complexity of the input–output dynamics to be controlled. The paper presents a model of the device and formulates some concise control problem statements for future research, along with illustrative simulation results. The case of single and dual bifurcation are presented.

1. Introduction

This article studies a class of prototype microfluidic systems exploiting the Zweifach-Fung effect to enrich or filter a fluid containing particles in suspension. Microfluidics is a vast scientific domain that emerged more than two decades ago [1]. It is commonly described as the science of manipulating and controlling fluids at Reynolds numbers under 1. Typical microfluidics devices are arranged in arrays of channels whose diameters are much smaller than 1 mm (from a few tens to a few hundreds of micrometers), see e.g. [2], and are designed to handle very small quantities (microliters to picoliters). Microfluidic systems are used in process engineering, chemistry, and biotechnology, among others, allowing fluids to interact, be mixed, measured, or encapsulated within each other, according to a desired process scheme. Typical networks of channels consist of inlets, zigzag, cross, split, traps, and pillars, among other architectures, see [3] for a state-of-the-art overview.

The fluid mechanics at stake in microfluidic systems is highly dependent on the complex geometry of the network. A phenomenon that has received particular attention in this field is the Zweifach-Fung effect (see [4]), a.k.a. *bifurcation law*. In words, it is described as follows, from [5]: "*when a suspension of particles reaches an asymmetric bifurcation, the particles volume fractions in the two daughter branches are not equal. In detail, for branches of comparable geometrical characteristics but receiving different flowrates, the volume fraction in particles increases in the high flowrate branch*".

The Zweifach-Fung effect has a central role in microvascular networks [6–10] and thus has been studied using in vivo, in vitro and theoretical models [11]. Interestingly, this effect can also serve to engineer sorting, fractionation or purification devices, see e.g. [12],[1] as is done in this article.

Many studies have concentrated on establishing empirical and theoretical laws describing the separation of particles in the two daughter branches of the main channel, using advanced models of computational fluid dynamics. Depending on various parameters such as widths, angles of the branches and size of particles, several semi-analytical laws have been proposed to describe the particle volume fraction in the two branches as a function of the flowrate ratios between them, see e.g. [13,14]. One can refer to [5] for a comprehensive analysis of these laws.

In this paper, we present several control problems on such systems. These problems are formulated on the simplest microfluidic set-up one can consider, pictured in Fig. 1. A main channel is used to transport a suspension contained in a (inlet) reservoir. Then, it reaches a bifurcation consisting of two equal dimension daughter branches. The bifurcation at stake is a T-shaped bifurcation (or a Y-shape, without loss of generality, see again [5]). The main channel and its daughter

E-mail address: nicolas.petit@minesparis.psl.eu.

[1] In such applications, quantities to be handled are very small. Typical channels have square section of 40 μm, lengths of 20 mm. Volumes to be treated are 30 μL over 30 min and the purification requirements are that concentration must be handled with an accuracy of 1%.

https://doi.org/10.1016/j.jprocont.2023.103124
Received 28 April 2023; Received in revised form 31 October 2023; Accepted 3 November 2023
0959-1524/© 2023 Published by Elsevier Ltd.

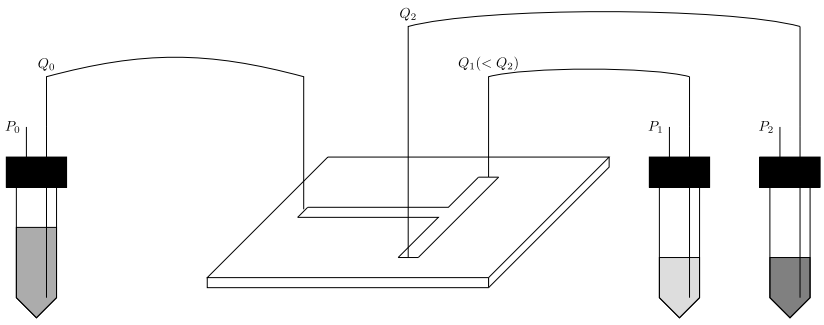

Fig. 1. Separation process using the Zweifach-Fung effect. A fluid containing particles flows from the inlet reservoir through a microfluidic device within which it reaches a bifurcation and finally flows to the outlet reservoirs. The flowrates Q_0, Q_1, Q_2 are controlled by the pressures P_0, P_1, P_2 in the reservoirs.

branches are contained in a single microfluidic chip. A two microfluidic chips setup is also considered in this article, to increase the fractionation efficiency.

In the control problems formulated in this article, the output of interest is the volume fraction in one of the output reservoirs, which can be controlled by changing the ratio between the flowrates of the daughter branches.

The paper is organized as follows. In Section 2 briefly details the model of the microfluidic chip, and presents a concise set of equations governing the system. The remarkable features of the dynamics is that it is nonlinear and subjected to an input-varying delay of hydraulic type. In Section 3, we discuss open-loop behavior and closed-loop stabilization. In Section 4, we consider a two-bifurcation system and generalize the findings of the preceding discussions. In Section 5 we describe several main challenges for application of optimization based techniques such as Model Predictive Control. Some conclusions and perspectives are given in Section 6.

2. Model of the dynamics

We first consider the single microfluidic chip system in Fig. 1. Note Q_0, Q_1, Q_2 the (volume) flowrates in the input, and two daughter (output) channels (1 and 2, respectively). For flows in microfluidic devices, liquids are well approximated as incompressible [15]. The fluid (suspension) contained in the reservoir consists of a solvent and particles. It is desired to increase the volume fraction of the fluid. The first branch is considered as a "waste channel" and the second branch is the "concentrated channel".

The inlet of the main channel and the outlets of the branches are connected through capillary tubings to three reservoirs. The reservoirs are pressurized with a high level of accuracy. The incompressibility of the fluid allows one to consider that the pressures at the ports are precisely controlled so that the flowrates can be chosen, almost instantly.[2] The ratio

$$u = \frac{Q_1}{Q_0} \in [0,\ 1]$$

is a control variable while Q_0 is kept constant. Conservation of volume implies that $Q_2 = Q_0 - Q_1$. When u is changed, the volume fraction after the bifurcation point is altered. Define c and $c\,f(u)$ the volume fraction in channel 0 and in channel 1 (right after the bifurcation), respectively. The mapping $u \mapsto f(u)$ is defined from the physical observations yielding the model below.

[2] Simple pressure controllers can be used in coordination with flowrate sensors for this purpose. The relationship between the flowrate and the pressure difference at the boundary of a channel is complex, but monotonic and smooth. See e.g. for discussions on these matters [16].

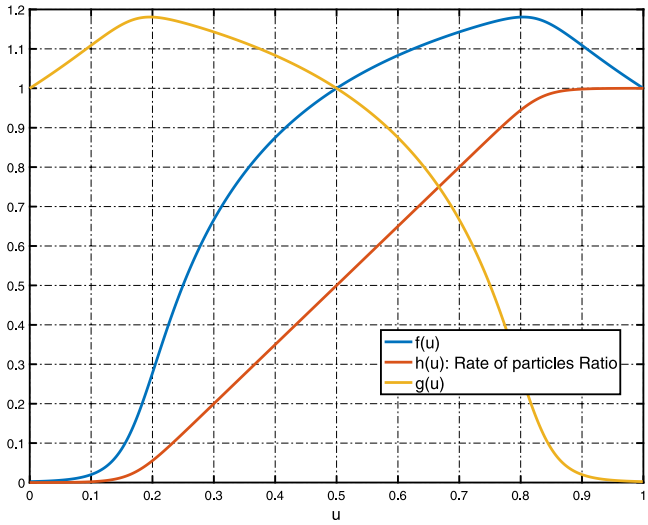

Fig. 2. The mapping f and the rate of particles ratio N_1/N_0.

Note N_0, N_1, $N_2 = N_0 - N_1$ the number of particles entering branches 0, 1 and 2, per unit of time, respectively. From experiments, see e.g. [12], one defines the mapping

$$u \mapsto N_1/N_0 \triangleq h(u)$$

such as pictured in Fig. 2 from data covering various cases of $Q_1/Q_2 = u/(1-u)$. This function stemming from experimental observations is the keystone to the model obtained below by simple balance and transport equations. A separation effect takes place because $h \neq \mathrm{Id}$. This mapping satisfies

$$h(u) + h(1-u) = 1$$

Noting $c\,g(u)$ the volume fraction in branch 2, one has

$$f(u) = \frac{h(u)}{u}, \quad g(u) = \frac{h(1-u)}{1-u} = \frac{1-u\,f(u)}{1-u} = f(1-u)$$

from which one readily obtains the conservation law

$$u f(u) + (1-u) g(u) = 1$$

The mapping f corresponding to the experimental data presented in [12] is illustrated in Fig. 2.

The outlet of channel 1 (waste channel) flows with no back mixing, into a reservoir. Consistently with the experimental constraints bearing on biological processes, a sensor measures the volume fraction of the fluid in this reservoir.[3]

[3] This allows to preserve the sterility of the fluid of interest in channel 2 (concentrated channel).

The waste channel reservoir contains a volume v of particles whose dynamics is

$$\dot{v} = c\, f(u(t - D(t)))\, Q_0\, u \tag{1}$$

where D is a *hydraulic delay* corresponding to the volume V_1 of channel 1 (from the bifurcation to the reservoir, through the capillary tubing). As for many systems involving transportation of material, see e.g. [17,18], this delay appears in the right-hand-side of the dynamics and is defined through an implicit integral equation.[4] In Eq. (1), this delay impacts the volume fraction as this quantity propagates without being altered in the channel (there is no back mixing), but it does not impact the flowrate which is uniform in the channel due to incompressibility. The implicit equation is

$$\int_{t-D(t)}^{t} u(\tau)d\tau = \frac{V_1}{Q_0} \tag{2}$$

The output of interest is the ratio of the volume fraction in the reservoir over the inlet volume fraction c. Assuming the reservoir is empty at $t = 0$, one has

$$y(t) = \frac{v}{c\, Q_0 \int_0^t u(\tau)d\tau} = \frac{\int_0^t f(u(\tau - D(\tau)))u(\tau)d\tau}{\int_0^t u(\tau)d\tau}$$

In practice, y can be measured. Typically, a cytometer is located at the outlet of channel 1, after the hydraulic delay. Tracking a reference value (setpoint) for y guarantees that the volume fraction in the two output reservoirs is maintained about a specific value of interest.

These notations allow us to formulate a first problem of practical interest for this microfluidic separation system.

Problem 1 (*Tracking of Volume Fraction in the Reservoirs*)**.** Consider the two states system $\dot{x}_1(t) = f(u(t - D(t)))u(t)$, $\dot{x}_2(t) = u(t)$, with single output $y(t) = x_1(t)/x_2(t)$, single input $u(t) \in [0, 1]$ and $D(t)$ defined by Eq. (2), find a closed-loop controller able to asymptotically stabilize any feasible setpoint y^{sp}.

Solving this problem has some practical interest in applications where the volume fraction plays a key role in the fluid dynamics at stake. These encompass biological suspension cultures [19], study of emulsion flows and droplet generation [20], high speed screening of biological reactions [21] among others.

3. Simulation, open-loop and closed-loop control

3.1. Numerical values for the model

The following values are used to produce the presented numerical results: $\frac{V_1}{Q_0} = 1$, f is represented in Fig. 2 and can be reproduced from the dataset detailed below in Section 3.2. Initial conditions[5] are $x_1(0) = x_2(0) = 0$. Past values of $u(t < 0)$ are uniform and set to 0.5.

3.2. Definition of f

The values of f over a finite uniform grid are given in Table 1. They are obtained from experimental data presented in [12]. When implementing these values, consistency with physical laws requires to forbid the interpolation to take negative values and it is necessary to enforce $f(0) = 0$, $f(0.5) = 1$, $f(1) = 1$. The mapping $u \mapsto f(u)$ is not defined outside $[0, 1]$.

[4] This equation stems from an exact solution of the transport partial differential equation with variable velocity, [17, Lemma 1.1].

[5] Arbitrary small values can be considered to avoid singularity in the numerical setup.

Table 1
Values of f for interpolation.

x	$f(x)$	x	$f(x)$
0	0.0		
0.0625	0.0077	0.5625	1.0556
0.1250	0.0412	0.6250	1.1000
0.1875	0.2194	0.6875	1.1364
0.2500	0.5011	0.7500	1.1663
0.3125	0.6999	0.8125	1.1801
0.3750	0.8333	0.8750	1.1370
0.4375	0.9285	0.9375	1.0662
0.5000	1.0	1	1.0

3.3. Numerical simulation

The responses of the system can be easily observed in numerical experiments, provided special care is taken in setting up the simulation solvers. To obtain reliable resolution of the input-dependent varying delay dynamics, special care is required on the numerical side as noted in [22]. A rich body of literature has long studied the numerical simulation of delay-differential algebraic equations (DDAE). Useful references can be found in [23,24] or [25]. A classic idea is to consider the underlying transport equation governing the system. Formally, this change of representation does not generate any approximation, Eq. (2) being the exact solution of the partial differential equation (PDE), see [26]. In turn this requires the discretization of the transport PDE.[6][7]

3.4. Open-loop behavior

Following the classic linear control design methodology (e.g. [28]), it is straightforward to apply various signals to the system and measure its open-loop responses. Such tests are reported in Fig. 3. For any input step-change, the open-loop response is monotonic. The response time and the delay depend on the final value of the step. In particular, for low values of the setpoint y^{sp}, a low value of the input $f^{-1}(y^{\text{sp}})$ has to be selected (according to the monotonicity of f for values below 0.5), and the delay gets large (according to the hydraulic nature of the delay Eq. (2)).

On overall, the open-loop responses reported in Fig. 3 are not satisfactory: the response is slow and the final error at the end of the considered time horizon is often large.

3.5. Closed-loop control

We are now interested in solving Problem 1 with closed-loop controllers.

3.5.1. Possible experimental apparatus for measurement and control

In practice, volume fraction y can be measured using several principles of detection such as electrical impedance, optical analysis and image analysis, [29,30]. These technologies are used in fluid and hematological analysis, and bacterial enumeration for example. Off the shelves devices are readily available from established manufacturers. Depending on the application and the technology at stake, reliable

[6] Good numerical schemes can be obtained using finite volumes methods. The approach described in [27] based on the use of the Method of Lines (MOL) by discretizing the PDE only with respect to space into a set of ordinary differential equations can be used. Comparable results can be obtained using a full discretization approach (both w.r.t. time and space) using a second order accurate scheme. It should be remembered that this type of finite volumes numerical schemes is stable only if the Courant–Friedrichs–Lewy condition is verified.

[7] An easy solution is the `Simulink Variable Time/Variable Delay` block set to "`Variable transport delay`" `delay type`.

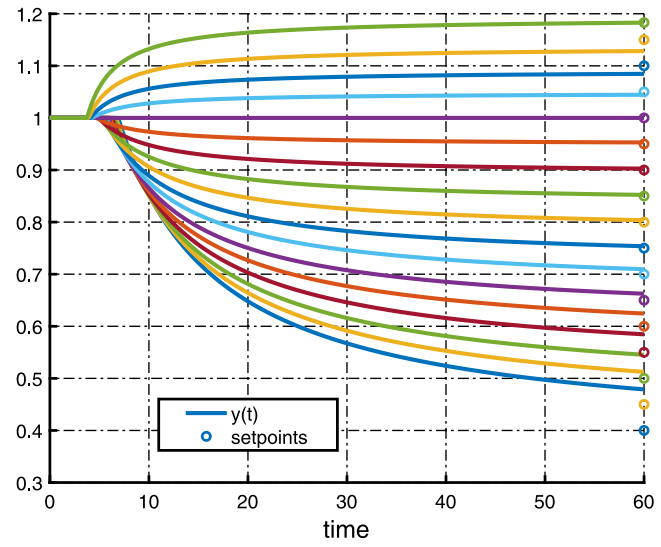

Fig. 3. Open-loop response to a step change in the input signal in hope to reach various references (one per color). Vertical axis y, lateral axis t (in s). The responses are monotonic. The response times and delays depend on the target reference. The final error at the end of the considered time horizon is large.

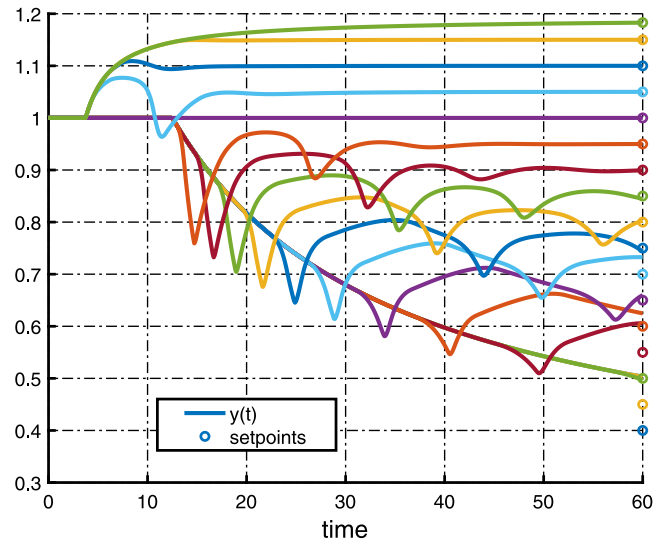

Fig. 4. Tracking of various references (one per color) with a PI with anti-windup. Vertical axis y, lateral axis t (in s). (note: the responses corresponding to the four smallest values of the setpoint are almost identical) A single a tuning gains does not grant a good level of performance on the whole range of interest.

measurements are produced at a relatively high rate. As already discussed the control variable u can be controlled using a flowrate sensor cascaded onto a pressure controller acting on the reservoirs. Several choices of sensors can be made, depending on the applications, the bandwidth requirements and the nature of the fluid (calorimetry-based, time-of-flight, Coriolis, or integrated optical fiber cantilever). Based on these principles, we explore the algorithmic solutions and pitfalls.

3.5.2. Stabilization by means of small gains PI

It is tempting to design a linear controller to improve the performance of the open-loop compensator. A natural first solution is a PI controller [31]. An example of performance obtained with a linear saturated controller (PI) is pictured in Fig. 4 for various step changes of the output setpoint. A single set of gains is used for all possible targets, and an anti-windup method [31] is implemented (here conditional integration). Some trade-off must be considered here to minimize undesired oscillations while limiting the final error in the response of the closed-loop system over the whole range of reachable set-points. The results presented here are one such optimal trade-off.

The results presented above are not fully satisfactory. Clearly, a single set of gains for the PI controller does not grant a good level of performance on the whole range of interest. This is mainly due to the varying nature of the hydraulic delay, the value of which directly depends on the values of the control itself.

3.5.3. Prediction based control

It is possible to account explicitly for the delay and its dependence, by means of a predictor, see [32–34]. Following the recent results in [35,36], one can formulate a general predictor for Problem 1 to assign the closed-loop behavior of the output of the system. The target dynamics is exponentially stable in a new time variable, which gives uniform exponential convergence in the real-world time (where the dynamics of the presented model are formulated) [36].

In a nutshell, see [36] for details and proof of convergence, with the notations of Problem 1, one has

$$\dot{y} = \frac{u}{Y}\left(f(u(t - D(t))) - y\right), \quad \dot{Y} = u \tag{3}$$

Consider

$$Y(t) = \int_0^t u(\ell)d\ell \tag{4}$$

Eq. (4) gives the delay through $r(t) = t - D(t)$, with

$$Y - Y \circ r = \frac{V_1}{Q_0} \tag{5}$$

so that

$$r = Y^{-1} \circ (Y - \frac{V_1}{Q_0}), \quad r^{-1} = Y \circ (Y + \frac{V_1}{Q_0})$$

According to Eq. (3), for any $k > 0$, the following nonlinear feedback gives exponential convergence (provided that u remains above some strictly positive constant) of y towards y^{sp}:

$$u \circ r = f^{-1}\left(y - k\,Y\,(y - y^{sp})\right)$$

giving $\dot{y} = -k\,u\,(y - y^{sp})$. This feedback has to be implemented in a causal form, in which it appears to be a predictor

$$u = f^{-1}\left(y \circ r^{-1} - k\,Y \circ r^{-1}\,(y \circ r^{-1} - y^{sp})\right)$$

From Eq. (5), one has $Y \circ r^{-1} = Y + \frac{V_1}{Q_0}$. The prediction $y \circ r^{-1} \triangleq P$ can be computed as follows. Conveniently, one can remark that

$$\dot{P} = \frac{dr^{-1}}{dt}\frac{u \circ r^{-1}}{Y \circ r^{-1}}\left(f(u) - y \circ r^{-1}\right)$$

Again, using Eq. (5), one has

$$\frac{dr^{-1}}{dt}\,u \circ r^{-1} = u$$

Therefore, one simply gets

$$\dot{P} = \frac{u}{Y + \frac{V_1}{Q_0}}\left(f(u) - P\right)$$

Finally, for improved numerical stability in the implementation, the predictor takes the following form (where W is an intermediate variable)

$$\dot{W} = \left(f(u(t)) - f(u(t - D(t)))\right)u(t)$$

$$\dot{Y} = u(t)$$

$$P(t) = \frac{y(t)Y(t) + W(t)}{Y(t) + \frac{V_1}{Q_0}}$$

$$u(t) = f^{-1}\left(P(t) - k\left(Y(t) + \frac{V_1}{Q_0}\right)\left(P(t) - y^{sp}\right)\right)$$

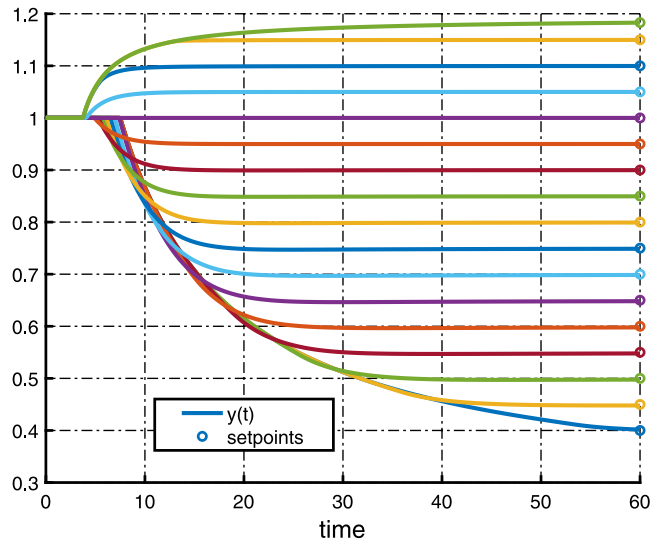

Fig. 5. Tracking of various references (one per color) with a predictor. Vertical axis y, lateral axis t (in s). A single value for the predictor gain grants a good level of performance on the whole range of interest.

When implemented, the predictor formula giving u is saturated.

Using this predictor, one obtains the closed-loop behavior[8] reported in Fig. 5. These results are significantly better compared to the ones obtained with a simple PI controller reported in Fig. 4.

3.5.4. Sampled measurement feedback

In view of future applications, a practical problem, simply stated below, is worth mentioning. The volume fraction measurement apparatus described above in Section 3.5.1 may have relatively long processing times, and can only treat fluid samples outside of the reservoir, causing an additional lag. Therefore, a formula representing these specifities and limitation is to model the measurement of y as follows

$$y^{\text{meas}}(t_i) = y(t_i - D_m(t_i)) + \varepsilon_i$$

where information is only available at instants t_i (forming an increasing sequence going to ∞, almost ideally spaced over a regular time grid) and $D_m(t_i)$ is a measurement delay, which can be considered as randomly distributed as in [37] or depending on the value of y itself as in [38,39]. A stochastic framework to model the noise ε_i is required, see e.g. [40]. The fact that the delay in the dynamics changes when the control changes complexifies significantly the analysis beyond what is usually considered, see e.g. [41].

4. Extension to multi-channel filtering

4.1. Model for two cascaded bifurcations

To maximize the fractionation capabilities, it is possible to cascade a second bifurcation at the outlet of the first one. The fluidic scheme is represented in Fig. 6 and schematized in Fig. 7.

The conservation laws serve to define the (volume) flow rates using three variables Q_0, Q_1 and Q_2. The flow rates Q_1 and Q_2 are controlled via the ratios

$$u_1 = \frac{Q_1}{Q_0} \text{ and } u_2 = \frac{Q_2}{Q_0 - Q_1}$$

where Q_0 is (usually) a constant. These flow rates define three hydraulic delays

$$\int_{r_1(t)}^{t} Q_0 u_1(\tau) d\tau = V_1, \quad \int_{r_{12}(t)}^{t} (Q_0 - Q_1(\tau)) d\tau = V_{12}, \quad \int_{r_2(t)}^{t} Q_2(\tau) d\tau = V_2$$

where V_1 and V_2 are the volume of the outlet branches after the first and second bifurcation, and V_{12} is the volume of the branch connecting the two bifurcations. One can make the dependency of the delays w.r.t. u_1 and u_2 more explicit

$$\int_{r_{12}(t)}^{t} (1 - u_1(\tau)) d\tau = V_{12}/Q_0, \quad \int_{r_2(t)}^{t} u_2(\tau)(1 - u_1(\tau)) d\tau = V_2/Q_0$$

The volume fraction upstream and downstream the first bifurcation are, as in the case of a single bifurcation, the triplet

$$c_1^{in} \triangleq c, \quad c_1^{in} f(u_1), \quad c_1^{out} \triangleq c_1^{in} \times \left(\frac{1 - u_1 f(u_1)}{1 - u_1} \right)$$

Upstream and downstream the second bifurcation they are

$$c_2^{in} \triangleq c_1^{out} \circ r_{12}, \quad c_2^{in} f(u_2), \quad c_2^{out} \triangleq c_2^{in} \times \left(\frac{1 - u_2 f(u_2)}{1 - u_2} \right)$$

The two upper branches of the bifurcations are connected to a single reservoir which contains a volume v of particles. By summing up the flow rates of particles of the two branches, $c_1^{in} f(u_1) \circ r_1 \times Q_1$ and $\left(c_2^{in} f(u_2)\right) \circ r_2 \times Q_2$ one obtains the variations of v as

$$\dot{v} = c\, f(u_1 \circ r_1)\, u_1\, Q_0 + c \times \left(\frac{1 - u_1\, f(u_1)}{1 - u_1} \right) \circ r_{12} \circ r_2 \times f(u_2 \circ r_2)\, u_2\, (1 - u_1)\, Q_0$$

The output of interest is the ratio of the volume fraction in the reservoir over the inlet volume fraction c. Assuming the reservoir is empty at $t = 0$, one has

$$y(t) = \frac{v(t)}{c\, Q_0 \int_0^t (u_1 + u_2 - u_1\, u_2)(\tau) d\tau}$$

4.2. Definition of a working point

For practical convenience, a single pressure controller is used in each outlet reservoir, which introduces a coupling of the flow in the two branches[9] Q_1 and Q_2 and

$$u_1 = u_2 \triangleq u$$

The flow rate of practical interest is $Q_f = Q_0 - Q_1 - Q_2$. At *equilibrium*,

$$Q_f = Q_0 (1 - u)^2$$

and the asymptotic separation properties of the system are defined by the ratio between the inlet volume fraction c and the outlet volume fraction

$$c \times \left(\frac{1 - u\, f(u)}{1 - u} \right)^2$$

The choice of a working point can be organized as follows, in accordance to Fig. 8. Considering that the production of interest of the system is a product with a higher volume fraction, a set of values for the concentration factor and flowrate are chosen by a user. This defines a unique value for u, from which the equilibrium of the measured output is determined. In the example pictured in Fig. 8 one has the following values, reported in Table 2.

[8] The open-loop behavior being Eq. (3).

[9] The microfluidic chips have different resistivity properties, to compensate for head losses.

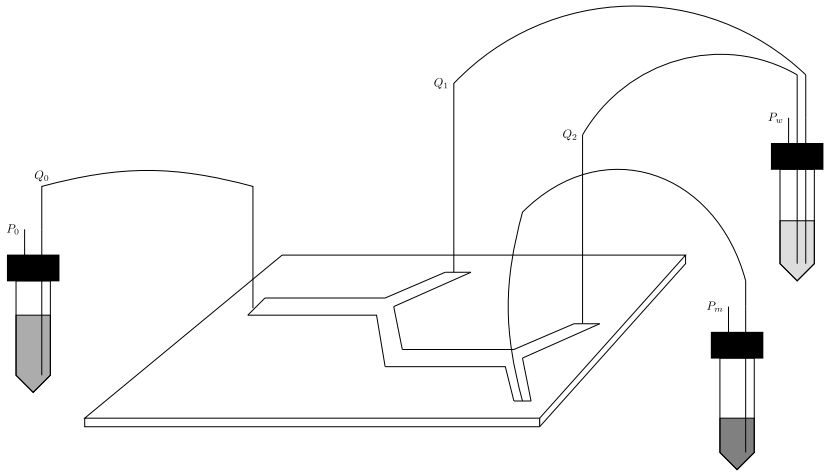

Fig. 6. Separation process using the Zweifach-Fung effect in two cascaded microfluidic chips to maximize the fractionation effect.

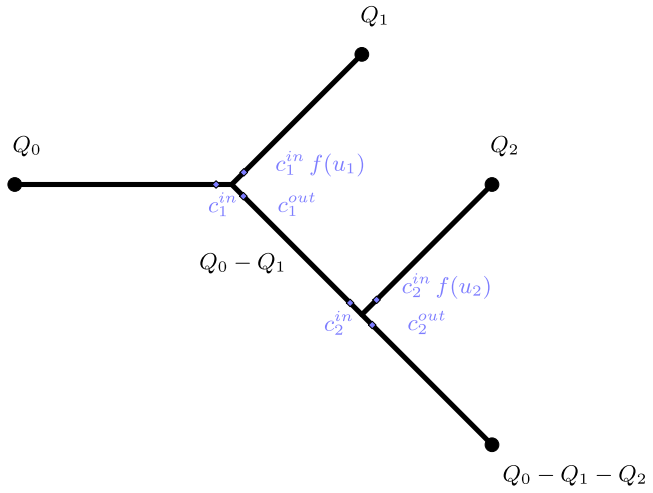

Fig. 7. Schematic representation of a dual bifurcation system.

Table 2
A fractionation working point for a dual bifurcation system.

Concentration factor	1.28
Flowrate (normalized)	46.2%
Waste flowrate (normalized)	53.8%
u	0.32
Measured output	0.76

4.3. Closed-loop control

These equations serve to define the following control problem.

Problem 2 (*Tracking of Volume Fraction for a Two-Bifurcation Device*)**.** Consider the two states system $\dot{x}_1 = f(u \circ r_1)\,u + \left(\frac{1-u\,f(u)}{1-u}\right) \circ r_{12} \circ r_2 \times f(u \circ r_2)\,u\,(1-u)$, $\dot{x}_2(t) = 2u(t) - u(t)^2$, with single output $y(t) = x_1(t)/x_2(t)$ and single input $u(t) \in [0,\ 1]$, and input varying delays $\int_{r_1(t)}^{t} u(\tau)d\tau = \frac{V_1}{Q_0}$, $\int_{r_{12}(t)}^{t}(1-u(\tau))d\tau = \frac{V_{12}}{Q_0}$, $\int_{r_2(t)}^{t} u(\tau)(1-u(\tau))d\tau = \frac{V_2}{Q_0}$, find a closed-loop controller able to asymptotically stabilize any feasible setpoint y^{sp}.

Numerical values for the model. In this section the following values are used in complement of the previous data. $\frac{V_1}{Q_0} = \frac{V_{12}}{Q_0} = \frac{V_2}{Q_0} = 1$, f is (unchanged and) represented in Fig. 2 and can be reproduced from the dataset reproduced in Section 3.2. Initial conditions[10] are $x_1(0) = x_2(0) = 0$. Past values of $u(t < 0)$ are uniform and set to 0.5.

The stabilization problem is to track a desired volume fraction in the waste reservoir using the single control variable u. As previously, a PI controller is used. In Fig. 9, we report a closed-loop behavior. The transient is similar to the one observed in Fig. 4 for a single bifurcation, but more erratic in appearance. Certainly, despite a careful tuning, the PI controller employed here is not the most appropriate to handle this system governed by the two hydraulic delays. By contrast, in Fig. 10 a predictor is used. To obtain the presented results, a very simple predictor was used, aiming at compensating only the *first* hydraulic delay $(t - r_1(t))$. It writes

$$\begin{aligned}
\dot{W} &= \left(f(u(t)) - f(u \circ r_1(t))\right) u(t) \\
\dot{Y} &= \left(f(u \circ r_1(t)) - Y\right) \frac{u(t)}{X} \\
\dot{X} &= u(t) \\
P(t) &= \frac{Y(t)X(t) + W(t)}{X(t) + V_1/Q_0} \\
u(t) &= f^{-1}\left(P(t) - k\left(X(t) + V_1/Q_0\right)\left(P(t) - y^{\text{sp}}\right)\right)
\end{aligned}$$

where k is a positive parameter defining the exponential convergence discussed above and y^{sp} is the output setpoint.[11] Other choices are possible. It is expected that a more complex prediction scheme compensating the three hydraulic delays of Problem 2 should be preferable. The formal analysis of the obtained tracking performance remains to be explored.

5. Optimization based-control

Optimization of the transient response of the system is motivated by the potentially extremely high value of the fluids that are processed by the device. A prime example of such case is when stem-cells are handled [42–44]. In many instances, the separation process is situated upstream the other operations. Very often the volume fraction is a critical parameter for subsequent operations. The fluid produced during the transient is not suitable for experiments and is considered lost. Examples of such situations include encapsulation processes [45], droplet generation [46], particle production [47] among others.

To minimize the loss, an optimal control approach seems like a natural solution.

[10] Arbitrary small values can be considered to avoid singularity in the numerical setup.

[11] When implemented, the predictor formula giving u is saturated.

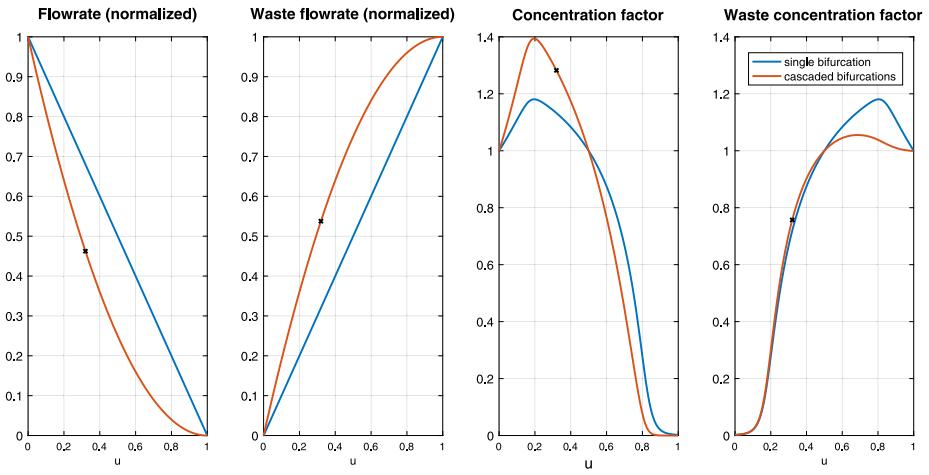

Fig. 8. Fractionation diagram for the single and dual bifurcation systems. The dual system offers a higher concentration factor.

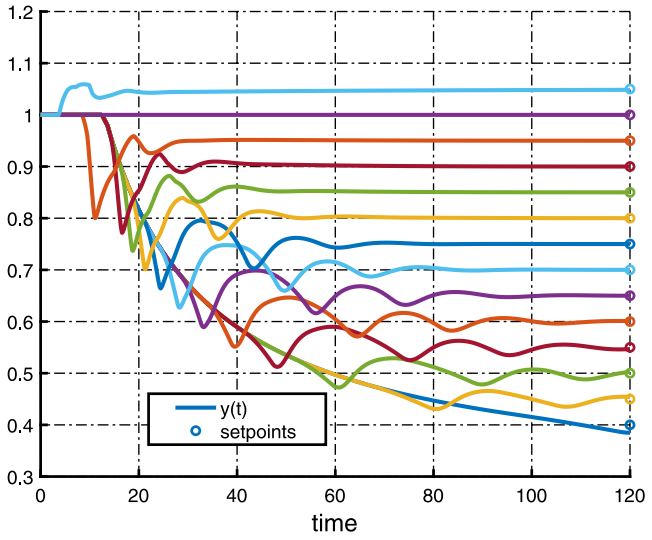

Fig. 9. Closed-loop performance on two bifurcations. Tracking of various references (one per color) with a PI with anti-windup. Vertical axis y, lateral axis t (in s). The transients have some spurious oscillations. A single set of tuning gains does not grant a good level of performance on the whole range of interest.

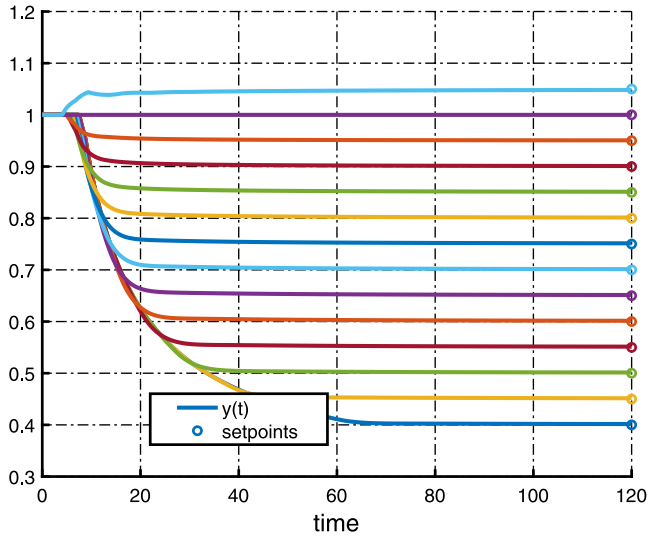

Fig. 10. Closed-loop performance on two bifurcations. Tracking of various references (one per color) with a predictor compensating only one of the delays. Vertical axis y, lateral axis t (in s). A single value for the predictor gain grants a good level of performance on the whole range of interest.

Considering the concise formulation of Problem 1, it is tempting to try to solve it with a classic Model Predictive Control methodology, see for example [48] for a typical application to a related problem. Besides the nonlinearity and controllability which is not straightforward as discussed below in Section 5.1, a more hidden pitfall is that any general optimal control problem formulated for the dynamics of Problem 1 is likely to be non smooth and will therefore reveal particularly troublesome for numerical solvers in its present form. This point is covered in Section 5.3.

5.1. Motion planning

The separation dynamics under consideration has some modeling similarities with the dynamics of dilution dynamics studied in other contexts [49]: hydraulic delays, binary graph as flow chart. Adding functions composition and inversion to the usual algebraic computation rules, it was shown in [49] that dilution systems are controllable in the sense of [50], i.e. that their trajectories can be explicitly parameterized in the sense of flat systems (see [51]) so that from a prescribed past trajectory on $]-\infty, 0]$ a trajectory can be constructed on $[0, T]$ for some $T > 0$ connecting to a future trajectory over $[T, +\infty[$. In dilution systems, the flat output under consideration is $Y(t)$ defined in (4).

For the separation systems studied in this paper, this variable also plays a key role to parameterize several of the variables at stake here. Indeed, in Problem 1, using Eq. (2), one gets $Y(t) - Y(t - D(t)) = \frac{V_1}{Q_0}$ which gives

$$D(t) = t - Y^{(-1)}(Y(t) - \frac{V_1}{Q_0})$$

which is valid as Y can be assumed strictly monotonic when $u > 0$, and thus is invertible. Here, the two additional states x_1 and x_2 of Problem 1 can be defined by integration (up to some initial condition) of right-hand sides solely defined by past values of Y.

$$\dot{x}_1 = f(\dot{Y}(Y^{(-1)}(Y(t) - \frac{V_1}{Q_0}))) \dot{Y}(t), \quad \dot{x}_2 = \dot{Y}(t)$$

to account for the initial conditions in the reservoir. Motion planning can be readily addressed by scheduling a smooth and monotonic trajectory for Y, the end points and the transient of which being determined according to the desired target in the reservoir.

As an illustration, Figs. 11 and 12 report open-loop histories obtained for a transient between two steady-states of the system over a

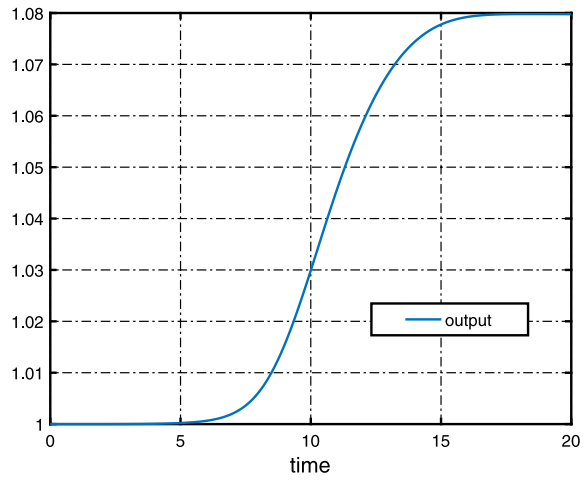

Fig. 11. Motion planning between two steady-states. The output y reaches a desired setpoint in finite-time.

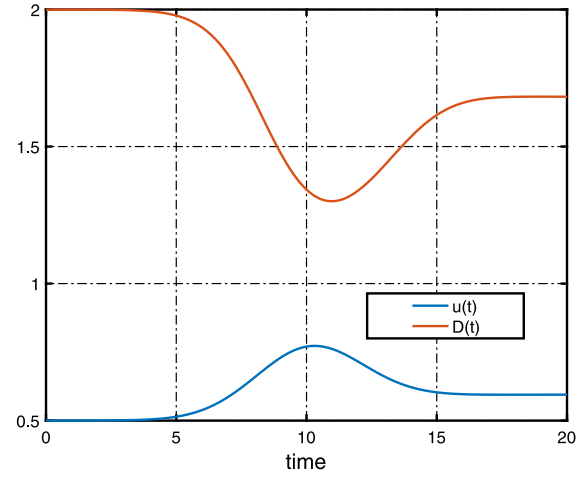

Fig. 12. Motion planning between two steady-states. The input u and the time varying-delay histories are reported.

finite time interval $[0, T]$. The matching condition

$$x_1(T) = f(u(T - D(T)))x_2(T)$$

is necessary to reach a steady-state. Numerous numerical methods can be employed to design an open-loop trajectory satisfying this condition, e.g. a Newton method on this condition using one or two parameters defining a set of candidate solutions.[12]

In practice this simple approach is only a first step, and optimal transients are desired. This is discussed next.

5.2. Two optimal control problems of practical interest

A first problem of practical interest is to reach a desired concentration in the reservoir in minimum time.

Problem 3 (*Reaching a Desired Reservoir Volume Fraction in Minimum Time*)**.** Consider the input–output description of Problem 1 and some initial conditions for x_1, x_2, and some past values for u and y^{sp}, solve $\min T$, where T is s.t. $y(T) = y^{\text{sp}}$.

[12] For reference, the numerical results where obtained for a value of $\frac{V_l}{Q_0} = 1$ with the same exact model previously defined, $T = 20$, $y(0) = 1$, $y(T) = 1.08$.

A second problem of interest expresses an optimal output tracking problem while limiting the variations of the control to account for the actuators limitations (pressure controllers are very fast but not infinitely fast). To formulate this, a state extension is considered.

Problem 4 (*Smoothly Reaching a Desired Reservoir Volume Fraction in Minimum Time*)**.** Consider the input–output description of Problem 1 and some initial conditions for x_1, x_2, and some past values for u and y^{sp}. Further consider the extra dynamic $\dot{u} = \omega$. Solve $\min_\omega \int_0^T ||y(t) - y^{\text{sp}}||^2 + \epsilon||\omega(t)||^2 dt$ for some fixed parameters $\epsilon > 0$ and $T > 0$.

5.3. Non smoothness related to hydraulic delays

Usually, potential solutions to optimal control problems are characterized by stationarity conditions. These conditions stem from the calculus of variations. The study of the calculus of variations for optimal control problems subject to time-varying delays in the dynamics is not a new subject. Main results are presented in [52,53], and can be seen as an extension to [54] given for fixed delays. Despite their generality, these results can not be applied to solve Problems 3 and 4. Indeed these works derive necessary stationarity conditions for delays depending once for all on t only and not on the state nor the control as is the case here.

The dependency of the delay on the input makes these results incomplete and some extra terms, possibly non-smooth appear. By expressing all the mutual interactions between the variables, it was shown in [55] under which conditions such an optimal control problem for a system subjected to a hydraulic delay is Gâteaux differentiable (see definition below in Proposition 1). It was also shown that this input dependency of the delay generally makes the system violate these conditions .

The general optimal control problem formulated in [56] is as follows. It covers Problems 3 and 4. We recall it to highlight the role of the delay dependency.

Let $\phi : \mathbb{R}^p \to \mathbb{R}_+^*$ be a smooth function, where p denotes the dimension of the variables. Without loss of generality, take some initial conditions (over a finite past) $(u_0, x_0) \in C^1_{ptw}([r_0; 0], \mathbb{R}^p) \times D^1([r_0; 0], \mathbb{R}^p)$ the class of piecewise continuously differentiable functions having a finite number of jumps in their values or derivatives on their interval of definition and the class of differentiable functions but whose derivative is not necessarily continuous, $r_0 < 0$ with $\int_{r_0}^0 \phi\left(u_0(\tau)\right) \mathrm{d}\tau = 1$. Consider the optimal control problem with input-dependent delays

$$\begin{aligned} \min_u & \int_0^T L(t, x(t), u(t))\,\mathrm{d}t + \psi(x(T)) \triangleq J_0(u) \\ s.t. \quad & \forall t \in [0; T],\ \dot{x}(t) = f(t, x(t), x(r_u(t)), u(t), u(r_u(t))) \\ & x_{[r_0;0]} = x_0,\ u_{[r_0;0]} = u_0 \end{aligned}$$

where r_u is defined by the relation $\int_{r_u(t)}^t \phi(u(\tau))\,\mathrm{d}\tau = 1$. The following result stresses the main issue of general non-differentiability. This property has to be understood in the sense of Gâteaux, recalled below, and requires the control to be continuous, which is sometimes in conflict with optimality. Below, for any function h of a real variable, we consider the one-sided limit whose s-argument defines how the t-argument is approached

$$\lim_{\substack{\tau \to t \\ s}} h(\tau) = \begin{cases} \lim_{\tau \to t^+} h(\tau) & \text{if} \quad 0 \le s \\ \lim_{\tau \to t^-} h(\tau) & \text{if} \quad 0 > s \end{cases}$$

Proposition 1. *Sensitivity of hydraulic delay w.r.t. input variations [56] For any $t \in [0; T]$, $(u, h) \in C^1_{ptw}([0; T], \mathbb{R}^p)^2$ and $s \in \{-1; 1\}$, we have*

$$\lim_{\substack{\delta \to 0 \\ s}} \frac{r_{u+\delta h}(t) - r_u(t)}{\delta} = \frac{1}{\lim_{\substack{\tau \to r_u(t) \\ s'}} \phi(u(\tau))} \int_{r_u(t)}^t \frac{\partial \phi}{\partial u}(u(\tau))h(\tau)\,\mathrm{d}\tau$$

where

$$s' = \operatorname{sign}\left(s \cdot \int_{r_u(t)}^{t} \frac{\partial \phi}{\partial u}(u(\tau))h(\tau)\,\mathrm{d}\tau \right)$$

In particular, if u is continuous at $r_u(t)$, the Gâteaux derivative of $r_u(t)$ w.r.t. the input at point u in the direction h is

$$D_h r_u(t) \triangleq \lim_{\delta \to 0} \frac{r_{u+\delta h}(t) - r_u(t)}{\delta} = \frac{1}{\phi(u(r_u(t)))} \int_{r_u(t)}^{t} \frac{\partial \phi}{\partial u}(u(\tau))h(\tau)\,\mathrm{d}\tau$$

Similarly, for any $t \in [0; r_u(T)[$

$$\lim_{\substack{\delta \to 0 \\ s}} \frac{r^{-1}_{u+\delta h}(t) - r^{-1}_{u}(t)}{\delta} = -\frac{1}{\lim_{\tau \to r^{-1}_u(t)_{s'}} \phi(u(\tau))} \int_{t}^{r^{-1}_u(t)} \frac{\partial \phi}{\partial u}(u(\tau))h(\tau)\,\mathrm{d}\tau$$

where

$$s' = \operatorname{sign}\left(-s \cdot \int_{t}^{r^{-1}_u(t)} \frac{\partial \phi}{\partial u}(u(\tau))h(\tau)\,\mathrm{d}\tau \right)$$

and if u is continuous at $r^{-1}_u(t)$ (which is not needed), the Gâteaux derivative is given by

$$D_h r^{-1}_u(t) = -\frac{1}{\phi(u(r^{-1}_u(t)))} \int_{t}^{r^{-1}_u(t)} \frac{\partial \phi}{\partial u}(u(\tau))h(\tau)\,\mathrm{d}\tau$$

with $r_u(t) = t - D(t)$.

This last expression can be checked to see the jumps. To circumvent the non-smoothness, it was suggested to introduce a regularized version of the problem and derive its stationarity conditions. The regularization can be shown to produce a sequence of solutions converging in a functional sense to the actual non-smooth solution when the regularization parameter is gradually reduced. Interestingly, this latter result can be seen as a refinement of the results of the pioneer work of [53] to the case of an hydraulic delay, under regularization. The sequence consists of fixed time-varying delayed optimal control problems. Each of these problems is defined using a sensitivity analysis stemming from the adjoint equations defined by the calculus of variations. A penalty term prevents the control from deviating too much between the two consecutive problems in the sequence, and a strong convexity results guarantees convergence. On the algorithm side, the resolution of the successive problems can be performed using a direct collocation transcription method (see e.g. [57]), with AMPL as algebraic modeling language and IPOPT as NLP solver (see details in [22]). Adjoint equations are resolved through a discretization scheme and used to formulate the next problem in the sequence.

Application of this technique to Problems 3 and 4 remains to be done.

6. Conclusion and perspectives

The purpose of this paper is to highlight a simple yet surprisingly rich and difficult to control class of nonlinear dynamics under input varying delay of hydraulic type. These microfluidic systems have some great interest in the community of lab-on-chips and there is little doubt that controlling it with a high level of performance, fast transients and strong disturbance rejection capabilities could be very beneficial in many situations where the handled fluids have very high costs. The predictor approach proposed in [35] provides very satisfying results. Formal analysis is out of the scope of the paper, we refer the interested reader to [35,36] for this point. In view of applications, it would be valuable to handle some uncertainty on the function f itself (while maintaining its constitutive properties of being positive, equal to 0 at $x = 0$ and equal to 1 at $x = 0.5$ and $x = 1$). Further, it is believed that a sophisticated predictor-based controller could be used for a cascade of such devices (a generalization of Problem 2), as the presented preliminary results suggest it, without proving it, and that predictors could be generalized to a cascade of arbitrary length of microfluidic chips. This will be the subject of further research.

Declaration of competing interest

The authors declare that they have no known competing financial interests or personal relationships that could have appeared to influence the work reported in this paper.

Data availability

No data was used for the research described in the article.

References

[1] N. Convery, N. Gadegaard, 30 Years of microfluidics, Micro Nano Eng. 2 (2019) 76–91.
[2] P. Tabeling, Introduction to Microfluidics, OUP Oxford, 2005.
[3] F. Paratore, V. Bacheva, M. Bercovici, G.V. Kaigala, Reconfigurable microfluidics, Nat. Rev. Chem. (2021) 1–11.
[4] Y. Fung, B. Zweifach, Microcirculation: Mechanics of blood flow in capillaries, Annu. Rev. Fluid Mech. 3 (1) (1971) 189–210.
[5] V. Doyeux, T. Podgorski, S. Peponas, M. Ismail, G. Coupier, Spheres in the vicinity of a bifurcation: Elucidating the Zweifach–Fung effect, J. Fluid Mech. 674 (2011) 359–388.
[6] Z. Shen, G. Coupier, B. Kaoui, B. Polack, J. Harting, C. Misbah, T. Podgorski, Inversion of hematocrit partition at microfluidic bifurcations, Microvasc. Res. 105 (2016) 40–46.
[7] A. Mantegazza, F. Clavica, D. Obrist, In vitro investigations of red blood cell phase separation in a complex microchannel network, Biomicrofluidics 14 (1) (2020) 014101.
[8] S. Roman, A. Merlo, P. Duru, F. Risso, S. Lorthois, Going beyond 20 μm-sized channels for studying red blood cell phase separation in microfluidic bifurcations, Biomicrofluidics 10 (3) (2016).
[9] Q. Zhou, J. Fidalgo, M.O. Bernabeu, M.S. Oliveira, T. Krüger, Emergent cell-free layer asymmetry and biased haematocrit partition in a biomimetic vascular network of successive bifurcations, Soft Matter 17 (13) (2021) 3619–3633.
[10] S.-S. Chang, S. Tu, K.I. Baek, A. Pietersen, Y.-H. Liu, V.M. Savage, S.-P.L. Hwang, T.K. Hsiai, M. Roper, Optimal occlusion uniformly partitions red blood cells fluxes within a microvascular network, PLoS Comput. Biol. 13 (12) (2017) 1–22.
[11] P. Balogh, P. Bagchi, Analysis of red blood cell partitioning at bifurcations in simulated microvascular networks, Phys. Fluids 30 (5) (2018).
[12] S. Yang, A. Ündar, J.D. Zahn, A microfluidic device for continuous, real time blood plasma separation, Lab Chip 6 (7) (2006) 871–880.
[13] J.W. Dellimore, M.J. Dunlop, P.B. Canham, Ratio of cells and plasma in blood flowing past branches in small plastic channels, Am. J. Physiol.-Heart Circul. Physiol. 244 (5) (1983) H635–H643.
[14] R. Guibert, C. Fonta, F. Plouraboué, A new approach to model confined suspensions flows in complex networks: Application to blood flow, Transp. Porous Media 83 (1) (2010) 171–194.
[15] B.J. Kirby, Micro-and Nanoscale Fluid Mechanics: Transport in Microfluidic Devices, Cambridge University Press, 2010.
[16] K.W. Oh, K. Lee, B. Ahn, E.P. Furlani, Design of pressure-driven microfluidic networks using electric circuit analogy, Lab Chip 12 (3) (2012) 515–545.
[17] D. Bresch-Pietri, N. Petit, Implicit integral equations for modeling systems with a transport delay, in: Recent Results on Time-Delay Systems, Springer, 2016, pp. 3–21.
[18] M. Chèbre, Y. Creff, N. Petit, Feedback control and optimization for the production of commercial fuels by blending, J. Process Control 20 (4) (2010) 441–451.
[19] R. Moloudi, S. Oh, C. Yang, K.L. Teo, A.T.-L. Lam, M. Ebrahimi Warkiani, M. Win Naing, Scaled-up inertial microfluidics: Retention system for microcarrier-based suspension cultures, Biotechnol. J. 14 (5) (2019) 1800674.
[20] A.D. Bick, S.K.Y. Tang, Effect of volume fraction on droplet break-up in an emulsion flowing through a microfluidic constriction, Appl. Phys. Lett. 115 (9) (2019) 093702.
[21] J.J. Agresti, E. Antipov, A.R. Abate, K. Ahn, A.C. Rowat, J.-C. Baret, M. Marquez, A.M. Klibanov, A.D. Griffiths, D.A. Weitz, Ultrahigh-throughput screening in drop-based microfluidics for directed evolution, Proc. Natl. Acad. Sci. 107 (9) (2010) 4004–4009.
[22] C.-H. Clerget, Contributions to the Control and Dynamic Optimization of Processes with Varying Delays (Ph.D. thesis), PSL University, 2017.
[23] H.T. Banks, F. Kappel, Spline approximations for functional differential equations, J. Differential Equations 34 (3) (1979) 496–522.
[24] A. Karoui, R. Vaillancourt, Computer solutions of state-dependent delay differential equations, Comput. Math. Appl. 27 (4) (1994) 37–51.
[25] U.M. Ascher, L. Petzold, The numerical solution of delay-differential-algebraic equations of retarded and neutral type, SIAM J. Numer. Anal. 32 (5) (1995) 1635–1657.

[26] D. Bresch-Pietri, Robust Control of Variable Time-Delay Systems. Theoretical Contributions and Applications to Engine Control (Ph.D. thesis), Mines ParisTech, 2012.
[27] A. Agarwal, Advanced Strategies for Optimal Design and Operation of Pressure Swing Adsorption Processes (Ph.D. thesis), Carnegie Mellon University, 2010.
[28] C.-T. Chen, Linear System Theory and Design, Saunders college publishing, 1984.
[29] K.M. McKinnon, Flow cytometry: An overview, Curr. Protocols Immunol. 120 (5.1) (2018) 1–11.
[30] Y. Han, Y. Gu, A.C. Zhang, Y.-H. Lo, Imaging technologies for flow cytometry, Lab Chip 16 (24) (2016) 4639–4647.
[31] K. Åström, T. Hägglund, The future of PID control, Control Eng. Pract. 9 (11) (2001) 1163–1175.
[32] D. Bresch-Pietri, J. Chauvin, N. Petit, Prediction-based stabilization of linear systems subject to input-dependent input delay of integral-type, IEEE Trans. Automat. Control 59 (9) (2014) 2385–2399.
[33] N. Bekiaris-Liberis, M. Krstic, Compensation of state-dependent input delay for nonlinear systems, IEEE Trans. Automat. Control 58 (2) (2012) 275–289.
[34] N. Bekiaris-Liberis, M. Krstic, Robustness of nonlinear predictor feedback laws to time-and state-dependent delay perturbations, Automatica 49 (6) (2013) 1576–1590.
[35] N. Bekiaris-Liberis, D. Bresch-Pietri, N. Petit, Predictor-feedback control of a model of microfluidic process with hydraulic input-dependent input delay, in: Proc. of the 2023 European Control Conference, 2023, pp. 2108–2113.
[36] N. Bekiaris-Liberis, D. Bresch-Pietri, N. Petit, Compensation of input-dependent hydraulic input delay for a model of a microfluidic process under Zweifach-Fung effect, Automatica to appear (2024).
[37] S. Kong, D. Bresch-Pietri, Constant time horizon prediction-based control for linear systems with time-varying input delay, IFAC-PapersOnLine 53 (2) (2020) 7665–7670.
[38] N. Bekiaris-Liberis, M. Krstic, Nonlinear control under delays that depend on delayed states, in: European Journal on Control, Special Issue for the ECC13, 2013.
[39] N. Bekiaris-Liberis, M. Krstic, Compensation of state-dependent input delay for nonlinear systems, IEEE Trans. Automat. Control (2013).
[40] H. Min, S. Xu, B. Zhang, Q. Ma, Output-feedback control for stochastic nonlinear systems subject to input saturation and time-varying delay, IEEE Trans. Automat. Control 64 (1) (2019) 359–364.
[41] H.-L. Choi, J.-T. Lim, Output feedback regulation of a chain of integrators with an unknown time-varying delay in the input, IEEE Trans. Automat. Control 55 (1) (2009) 263–268.
[42] H.-W. Wu, C.-C. Lin, G.-B. Lee, Stem cells in microfluidics, Biomicrofluidics 5 (1) (2011).
[43] W. Zhang, K. Kai, D.S. Choi, T. Iwamoto, Y.H. Nguyen, H. Wong, M.D. Landis, N.T. Ueno, J. Chang, L. Qin, Microfluidics separation reveals the stem-cell–like deformability of tumor-initiating cells, Proc. Natl. Acad. Sci. 109 (46) (2012) 18707–18712.
[44] Q. Zhang, R.H. Austin, Applications of microfluidics in stem cell biology, BioNanoScience 2 (4) (2012) 277–286.
[45] Q. Wang, Q. Liu, L.-L. Fan, L. Zhao, The formation of droplet encapsulating particles in a Y-typed microchannel, Measurement: Sensors 14 (2021) 100039.
[46] Z. Nie, W. Li, M. Seo, S. Xu, E. Kumacheva, Janus and ternary particles generated by microfluidic synthesis: design, synthesis, and self-assembly, J. Am. Chem. Soc. 128 (29) (2006) 9408–9412.
[47] Z. Liu, F. Fontana, A. Python, J.T. Hirvonen, H.A. Santos, Microfluidics for production of particles: mechanism, methodology, and applications, Small 16 (9) (2020) 1904673.
[48] M. Sbarciog, R. De Keyser, S. Cristea, C. De Prada, Nonlinear predictive control of processes with variable time delay. A temperature control case study, in: 2008 IEEE International Conference on Control Applications, IEEE, 2008, pp. 1001–1006.
[49] N. Petit, Y. Creff, P. Rouchon, Motion planning for two classes of nonlinear systems with delays depending on the control, in: Proc. of the 37th IEEE Conference on Decision and Control, 1998, pp. 1007–1011.
[50] J.C. Willems, Paradigms and puzzles in the theory of dynamical systems, IEEE Trans. Autom. Control 36 (3) (1991) 259–294.
[51] M. Fliess, J. Lévine, P. Martin, P. Rouchon, A Lie-Bäcklund approach to equivalence and flatness of nonlinear systems, IEEE Trans. Autom. Control 44 (5) (1999) 922–937.
[52] H.T. Banks, Necessary conditions for control problems with variable time lags, SIAM J. Control 6 (1) (1968) 9–47.
[53] R.B. Asher, H.R. Sebesta, Optimal control of systems with state-dependent time delay, Internat. J. Control 14 (2) (1971) 353–366.
[54] D.K. Hughes, Variational and optimal control problems with delayed argument, J. Optim. Theory Appl. 2 (1968) 1–14.
[55] C.-H. Clerget, N. Petit, Optimal control of systems subject to input-dependent hydraulic delays, IEEE Trans. Automat. Control 66 (1) (2020) 245–260.
[56] C.-H. Clerget, N. Petit, Dynamic optimization of processes with time varying hydraulic delays, J. Process Control 83 (2019) 20–29.
[57] L.T. Biegler, Solution of dynamic optimization problems by successive quadratic programming and orthogonal collocation, Comput. Chem. Eng. 8 (3–4) (1984) 243–247.